Journal of Data Acquisition and Processing
ISSN: 1004-9037
https://sjcjycl.cn/
DOI: 10.5281/zenodo.98549558

COMPARATIVE STUDY OF HHO-PI USING MODULAR MULTILEVEL CONVERTER-BASED UPFC SYSTEM

Tejaswini.B
Research Scholar, Department of Electrical and Electronics Engineering, Dr.M.G.R Educational and Research Institute, Maduravoyal, Chennai – 95, India

E.Sheeba Percis
Professor, Department of Electrical and Electronics Engineering, Dr.M.G.R Educational and Research Institute, Maduravoyal, Chennai – 95, India

ABSTRACT
This research study presents a comprehensive comparative analysis of two controllers, namely the HHO-PI and PI, for regulating the DC link voltage of a Unified Power Flow Controller.The objective was to assess the action of these controllers in terms of transient response, robustness, power flow control, and power quality. The results show that the HHO-PI controller outperforms the PI controller in terms of transient response, robustness, power flow control, and power quality. The HHO-PI controller's hybrid harmony search optimization algorithm enhances optimization capabilities, leading to improved performance in adapting to changing operating conditions and maintaining a stable DC link voltage. It also achieves smoother tracking of active and reactive power references, resulting in better power flow management and increased system stability. The HHO-PI controller yields significantly lower Total Harmonic Distortion (THD) values, indicating improved power quality. These findings highlight the superiority of the HHO-PI controller for UPFC systems.
Keywords—UPFC system, HHO-PI, modular multilevel converter, etc.

I. INTRODUCTION
Power quality issues, including harmonics and voltage stability, have become significant concerns in modern smart grids due to the increasing penetration of nonlinear loads*(Debnath et al., 2015)*. Nonlinear loads, such as electronic devices and power electronic converters, introduce harmonics into the power system, leading to undesirable effects such as increased losses, reduced efficiency, and potential damage to equipment*(Perez et al., 2021)*. Moreover, voltage stability is crucial for the reliable operation of power systems and the quality of electrical supply to consumers*(Perez et al., 2021)*. In order to address these difficulties, we need solutions that are both effective and efficient, and which can reduce the amount of current source harmonics while keeping the voltage as stable as possible under a variety of loading scenarios *(Zeng & Xu, n.d.)*. Although filters have traditionally been used for harmonics elimination, their high cost and limited dynamic performance make them impractical for achieving desired results across a wide range of loading scenarios*(Alabool et al., 2021)*.
The UPFC is a flexible power electronic device that integrates both series and shunt converters, enabling the precise control of power flow and voltage at the common coupling point *(Thamizh Thentral et al., 2021)*. To reduce source current harmonics, we employ the (DDSRF) theory, it results in the generation of sinusoidal harmonics that have phases that are opposite to those of

the load current. By injecting or absorbing reactive power at the PCC, the UPFC actively compensates for the harmonics introduced by nonlinear loads, minimizing their impact on the power system*(Thentral et al., 2022)*. To ensure accurate and responsive control, a hysteresis controller is employed to generate Pulse Width Modulation (PWM) pulses for the shunt and series compensators once the DDSRF theory is applied*(Kamal et al., 2022)*. This control strategy allows for real-time adjustment of the UPFC parameters, enabling rapid and efficient harmonic mitigation*(Patel & Talari, 2021)*.

The key advantage of utilizing the DDSRF theory lies in its potential to achieve maximum voltage stability while minimizing source current harmonics under diverse loading circumstances*(Meral & Çelik, 2019)*. By injecting or absorbing reactive power at the common coupling point (CCP), the UPFC can effectively improve the overall power quality and mitigate the impact of nonlinear loads on the grid*(Alexander Jeevanantham & Srinath, 2022)*. To control the UPFC and implement the DDSRF theory, a hysteresis controller is employed to generate pulse width modulation (PWM) pulses for the shunt and series compensators*(He et al., 2019)*. The DDSRF theory is also compared to the existing dq theory in terms of Total Harmonic Distortion (THD) analysis to evaluate its effectiveness and performance*(Heenkenda et al., 2023)*.

Additionally, the capacitor DC link voltage, a critical parameter in the operation of the UPFC, is regulated using a Proportional-Integral-Derivative (PID) controller*(Tripathy et al., 2022)*. To optimize the PID controller's gain parameters, the Harris Hawks Optimization (HHO) technique is employed, ensuring efficient and stable voltage control in the system*(Gupta, 2022)*. Through this research, the effectiveness and efficiency of the proposed UPFC system with DDSRF theory will be demonstrated, focusing on voltage stability and source current harmonics reduction*(Xiu et al., 2021)*. By providing a comprehensive solution to power quality problems in smart grids, this research contributes to the overall improvement of grid performance and reliability in the face of increasingly complex and nonlinear loads*(Roknuzzaman et al., 2020)*.

II. BACKGROUND

Modular multi-level converters (MMCs), that are used to both greatly increase the voltage that is produced quality and significantly lower the recommended voltage of switching devices, have received a lot of attention in research throughout time.*(Perez et al., 2021)*. These converters have been the primary focus of their interest*(Reddy et al., 2021)*.MMC is being promoted as a superior alternative for variable speed drive systems, high-voltage DC gearbox systems, and specialist power devices *(Gade et al., 2021)*. Shunt converters and series converters are not the same thing; They both consist of Submodules with a full-bridge or a half-bridge, and operate in a different way*(Zeng & Xu, n.d.)*. To reach an output voltage level equal to (2 N + 1), Two N half-fridge submodules make up the shunt + series converter. *(Choudhury et al., 2021)*.

A. MMC (Modular Multilevel Converter)

figure. 1shows It comprises of three stages of units, with an arm reactor connecting each phase's top and bottom bridges AC line u_{si} (i = a, b, c). An L-shaped inductance and a resistor R_s,

combined are analogous to the arm reactorx, where i_{si} , i_{pi} , and i_{ni} are the upper or lower bridge phases' arm currents, respectively, and i_{dc} is the grid's ac current.

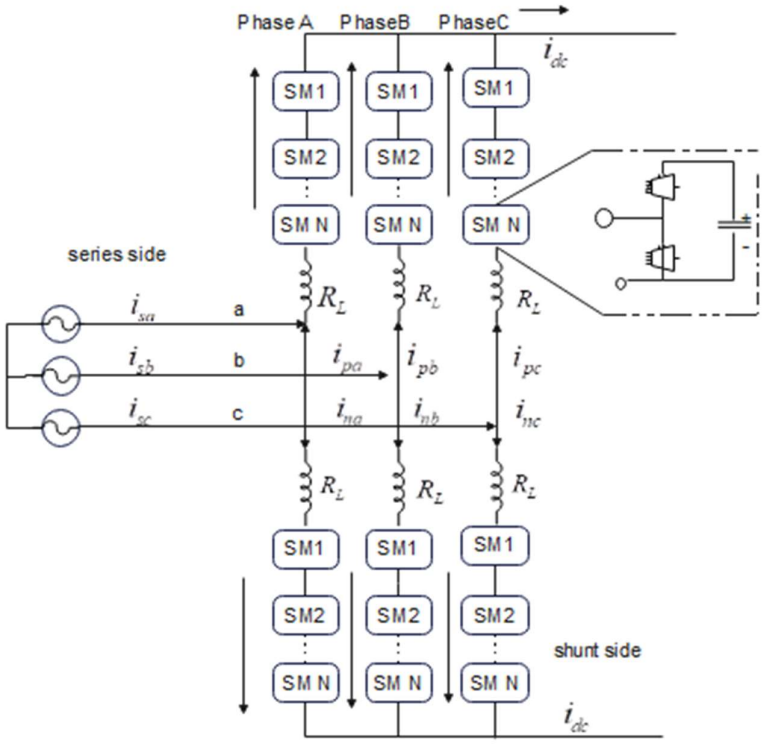

Figure 1 MMC based Series converter

An individual block's potential difference is denoted by the symbol u_{sm} ; the The top and bottom subblocks' dc capacitor voltages are represented by the symbols u_{smp} and u_{smn} respectively. A shunt connection is made between the capacitor of each and every sub block and the equivalent resistor R_P so that the sub block may be simulated. If we assume that the leading edge of the top bridges arm or the tip of the bottom bridges will meet at the corresponding potential point, if we disregard the arm resistor, and if we put the potential into u_{oi} (i = a, b, c), then its connections may be shown in Fig. 2. The lower arm's DC potential is denoted by $\frac{u_{dc}}{2}$, while the voltage between the bottom and upper arms is denoted by u1dsiandu2dsi respectively. During a switch cycle, the top and bottom arm blocks' respective duty cycles are denoted by d_{pi} and d_{ni} respectively. The ac power is denoted by u_{si} .

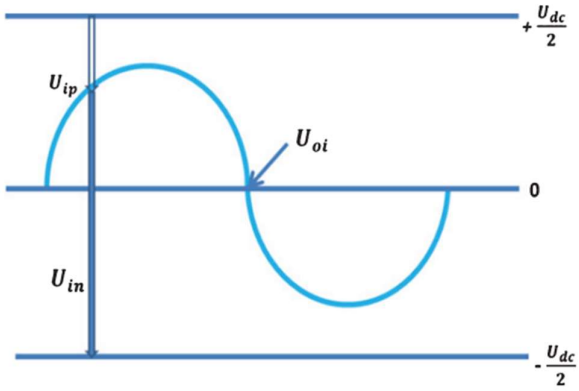

Figure 2Connections between MMC's bridge, alternating, and direct currents

T_s and $\overline{xT_s}$ are the During a switching cycle, the average values of the electric parameter x sT_s . T_s is the switching cycle time? The upand down arm switching models the MMC may be generated by using the KVL Law, and these models are shown below.

$$\frac{\overline{di_{piTs}}}{dt}=\frac{1}{L}(\overline{-u_{1\Delta d_{si}T_s}}+d_{pi}\overline{Nu_{smpTs}}-R_s\overline{i_{piT_s}}) \quad (1)$$

$$\frac{\overline{du_{smpTs}}}{dt}=\frac{1}{C}(-d_{pi}\overline{i_{piTs}}-\frac{\overline{u_{smpTs}}}{R_p}) \quad (2)$$

$$\frac{d\overline{i_{niTs}}}{dt}=\frac{1}{L}(\overline{u_{2\Delta dsiTs}}-R_s\overline{i_{niTs}}) \quad (3)$$

$$\frac{\overline{du_{smnTs}}}{dt}=\frac{1}{C}(d_{ni}\overline{i_{niTs}}-\frac{\overline{u_{smnTs}}}{R_n}) \quad (4)$$

Given the proportions of the capacitor voltage and the top & bottom bridging arm variables, and assuming $R_p = R_n = R$, $u_{smp} = u_{sm}$, we obtain by adding (1) and (2).

$$\frac{d\overline{i_{siTs}}}{dt}=\frac{1}{L}(\overline{u_{siTs}}+N(d_{ni}-d_i)\overline{u_{smTs}}-R_s\overline{i_{siTs}}) \quad (5)$$

$$\frac{d\overline{u_{smTs}}}{dt}=\frac{1}{2C}(d_i\overline{i_{niTs}}-d_{piTs})-\frac{\overline{u_{smTs}}}{RC} \quad (6)$$

In the formula above, i_{si} represents $i_{si}+i_{ni}$, and u_{si} represents $u_{si}+u_{ni}$. The relationship may be found by adding the output voltages of the up and down arms in subblock.

$$Nd_{pi}\overline{u_{mTs}}=\overline{u_{dc}/2_{Ts}}-\overline{u_{oiTs}} \quad (7)$$

$$Nd_{ni}\overline{u_{mTs}}=\overline{u_{dc}/2_{Ts}}-\overline{u_{oiTs}} \quad (8)$$

During the process of developing the model, without taking into account the reactive voltage in arm, u_{dc} was found to be greater than N_{usm}. As a result, according to formula (4), d_{pi} and d_{ni} satisfied the requirements of formula (5).

$$d_{pi} = \frac{1}{2}(1 - d_i) \tag{9}$$

$$d_{ni} = \frac{1}{2}(1 - d_i) \tag{10}$$

di refers to each stage's equivalent output modulating cycle. In order to continue with the parameter replacement in equations (3), The MMC system's usual switching cycle is required.

$$\frac{d\overline{i_{siTs}}}{dt} = \frac{1}{L}(2\overline{u_{siTs}} + Nd_i\overline{u_{smTs}} - R_s\overline{i_{siTs}}) \tag{11}$$

$$\frac{d\overline{u_{smTs}}}{dt} = \frac{1}{2C}(\frac{di}{2}\overline{i_{siTs}} - \frac{i_{dc}}{3} - \frac{\overline{u_{smTs}}}{RC}) \tag{12}$$

It is feasible to determine the usual switching cycle for the MMC in the dq framework by using Park's transformation.

$$\frac{L}{2}\frac{d\overline{i_{sdTs}}}{dt} + \frac{R_s}{2}\overline{i_{sdTs}} = \overline{u_{sdTs}} + \frac{\omega L}{2}\overline{i_{sqTs}} - \frac{N\overline{u_{smTs}}.d_d}{2} \tag{13}$$

$$\frac{L}{2}\frac{d\overline{i_{sqTs}}}{dt} + \frac{R_s}{2}\overline{i_{sqTs}} = \overline{u_{sqTs}} + \frac{\omega L}{2}\overline{i_{sqTs}} - \frac{N\overline{u_{smTs}}.d_q}{2} \tag{14}$$

$$6C.\frac{d\overline{u_{mTs}}}{2} = \frac{3}{4}(\overline{d_d.i_{sd} + d_q.i_{sq}})Ts - i_{dc} - \frac{6\overline{u_{smTs}}}{R} \tag{15}$$

B.Harris Hawks Optimization (HHO)

A Proportional-Integral-Derivative (PID) controller's gain parameters can be adjusted using the HHO method. The PID controller is a widely used control algorithm in a wide range of industries and applications. Its goal is to regulate the output of a system by altering the amount of control effort according to the difference between what is wanted and the actual result.The HHO algorithm was inspired by Harris hawk hunting behaviours, can be used as an optimisation method to find the best gain parameter amounts for the PID controller By applying the HHO algorithm, the search for the best set of PID gains is performed in the solution space, where each candidate solution represents a unique combination of Gains that are proportional, integral, or derivative.

Algorithm 2: The Procedure of HHO

1: **Commence** (N) search agents (yi ; i $\mathcal{E}$(1:N))

2: **While T isn't reached yet**

3: **Estimate** the fitness of the solutions

4: **Find** the global best solution (y_{rabbit})

Asses the escaping energy (E) as in Eq. 6.
If $(|E| \geq 1)$ Then
Update the movement according to Eq. 7
Else
If $(|E| \geq 0.5)$ and $(|r| \geq 0.5)$ Then
Update the location according to Eq. 8
Else If $(|E| \geq 0.5)$ and $(|r| < 0.5)$ Then
Update the location according to Eq. 9 to Eq. 12
Else If $(|E| < 0.5)$ and $(|r| \geq 0.5)$ Then
Update the location according to Eq. 13
Else
Update the location according to Eq. 14 to Eq. 16
EndIf
EndIf
Iterate step (6) for (N) search agents
EndWhile
Produce (y_{rabbit}) as the global best solution

III. PROPOSED SYSTEM DESIGN

Shunt or series converters make up the two converters that make up the planned UPFC. A series transformer connects the arrangement compensator to the line. The capacitor stores the DC potential that was converted from AC potential by this converter. The shunt converter transforms the DC potential that has been stored into alternating potential in three phases. The possibility flows to the linear load through a transformer. The DDSRF theory employs the voltage of the supply and current to produce the reference flow. hysteresis controller analyses actual with reference voltages to produce a PWM signal. The shunt converter receives the PWM signal. Essentially, a comparison is made between the reference voltage and the measured potential, where the result is a PWM signal, which is maintained to the arrangement converter. The PI controllers use an arrangement converter to keep the capacitor's DC potential

constant. The UPFC design achieves potential & flow remuneration through the use of shunt and series compensators. Opposing overtones are fed into the PCC by a shunt converter.

In this study, the Integral Time-weighted Absolute Error (ITAE) is employed as a performance criterion to fine-tune the (PID) controller. The primary objective is to optimize the controller's parameters in order to minimize the ITAE.

Objective Function:

$$\int_{0}^{Ts} \left| V_{link}^{ref} - V_{link}^{actual} \right| \qquad (16)$$

Where,

Ts → Simulation time

V_{link}^{ref} → Reference DC-link voltage

V_{link}^{actual} → Actual DC-link voltage

Based on the ITAE calculation, an optimization algorithm is employed to adjust the parameters (K_p and K_i). The goal is to minimize the ITAE, which indicates a better control system performance. The Harris Hawks optimization (HHO) technique is used to regulate the PID controller's gain parameters.The optimization algorithm iteratively adjusts the controller parameters and evaluates the resulting ITAE until convergence or the desired performance is achieved.

The adjusted PID controller settings are transmitted to the management system after the optimisation procedure is finished. Various criteria are used to assess the control system's performance, including tracking accuracy, stability, or response time. To evaluate the durability of the adjusted controller under various operating situations, a sensitivity study may also be used.

Overall, by utilizing the ITAE to tune the PID controller, this study aims to enhance the control system's performance and achieve improved tracking of the desired response. The ITAE serves as an objective criterion to guide the parameter optimization process, enabling the selection of optimal PI controller settings for the specific control system under investigation.

A. Proposed DDSRF theory modelling for UPFC system

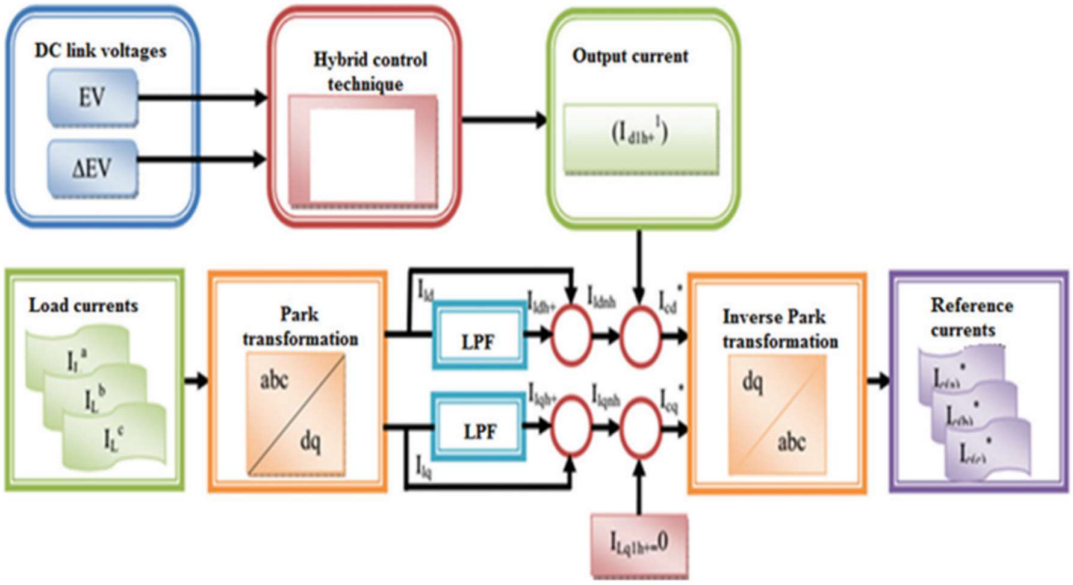

Figure 3 DDSRF modelling of UPFC system

The theoretical DDSRF modelling for the suggested UPFC system. The components of the three-phase current alternating potential are the positive, the negative, and zero sequence.

$$\begin{bmatrix} V_{sa} \\ V_{sb} \\ V_{Sc} \end{bmatrix} = V_a \begin{bmatrix} \cos(\omega t + \varphi_0) \\ \cos(\omega t + \varphi_0) \\ \cos(\omega t + \varphi_0) \end{bmatrix} + V_b \begin{bmatrix} \cos(\omega t + \varphi_1) \\ \cos(\omega t - \frac{2\pi}{3} + \varphi_1) \\ \cos(\omega t + \frac{2\pi}{3} + \varphi_1) \end{bmatrix} + V_c \begin{bmatrix} \cos(\omega t + \phi_2) \\ \cos(\omega t + \frac{2\pi}{3} + \phi_2) \\ \cos(\omega t - \frac{2\pi}{3} + \phi_2) \end{bmatrix} \quad (17)$$

Where V_{sa}, V_{sb}, and V_{sc} are phase alternating current voltages, V_a, V_b, and $V_c$are both positive and negative voltage sequences.

$$V_s = \begin{bmatrix} V_{sa} \\ V_{sb} \\ V_{sc} \end{bmatrix} = \begin{bmatrix} V_{a0} \\ V_{b0} \\ V_{c0} \end{bmatrix} + \begin{bmatrix} V_{a1} \\ V_{b1} \\ V_{c1} \end{bmatrix} + \begin{bmatrix} V_{a2} \\ V_{b2} \\ V_{c2} \end{bmatrix} \quad (18)$$

The source of three-phase current is depicted as,

$$I_S = \begin{bmatrix} I_{Sa} \\ I_{Sb} \\ I_{Sc} \end{bmatrix} = \begin{bmatrix} I_{a0} \\ I_{b0} \\ I_{c0} \end{bmatrix} + \begin{bmatrix} I_{a1} \\ I_{b1} \\ I_{c1} \end{bmatrix} + \begin{bmatrix} I_{a2} \\ I_{b2} \\ I_{c2} \end{bmatrix} \quad (19)$$

The perceived authority is denoted by

$$S_S = P_s + j\,Q_S = V_S I_S^* \quad (20)$$

The general equation for DDSRF theory is given as,

$$S_{s012} = P_{I012} + S_{f012} \quad (21)$$

The entire quantity of energy entering the grid is determined as 0, 1, and 2, which represent the zero, favourable, and negative sequencing powers, respectively,

$$S_{1012} = P_{s012} + S_{h012} \tag{22}$$

$$S_{1012} = P_{s012}(t) + Q_{s012}(t) + P_{h012}(t) + Q_{h012}(t) \tag{23}$$

P and Q are abbreviations that stand for the system's active and responsive powers, respectively.

The input a three-phase voltage and fluxes are transformed using a Clark transformation to variables having a value of 0.

$$V_{\alpha\beta 0} = \frac{2}{3}\begin{bmatrix} 1 & -\frac{1}{2} & -\frac{1}{2} \\ 0 & \frac{\sqrt{3}}{2} & -\frac{\sqrt{3}}{2} \\ \frac{1}{2} & \frac{1}{2} & \frac{1}{2} \end{bmatrix} V_s$$

$$I_{\alpha\beta 0} = \frac{2}{3}\begin{bmatrix} 1 & -\frac{1}{2} & -\frac{1}{2} \\ 0 & \frac{\sqrt{3}}{2} & -\frac{\sqrt{3}}{2} \\ \frac{1}{2} & \frac{1}{2} & \frac{1}{2} \end{bmatrix} I_s$$

The parameters are estimated from above equation,

$$V_{\alpha\beta} = \frac{2}{3}\begin{bmatrix} 1 & -\frac{1}{2} & -\frac{1}{2} \\ 0 & \frac{\sqrt{3}}{2} & -\frac{\sqrt{3}}{2} \end{bmatrix} V_s$$

$$I_{\alpha\beta} = \frac{2}{3}\begin{bmatrix} 1 & -\frac{1}{2} & -\frac{1}{2} \\ 0 & \frac{\sqrt{3}}{2} & -\frac{\sqrt{3}}{2} \end{bmatrix} I_s$$

Variables are estimated from the positive & negative sequence elements,

$$V_{\alpha\beta} = V_1\begin{bmatrix} \cos(\omega t + \varphi_1) \\ \sin(\omega t + \varphi_1) \end{bmatrix} + V_2\begin{bmatrix} \cos(\omega t + \varphi_2) \\ \sin(\omega t + \varphi_2) \end{bmatrix}$$

$$V_{dq1} = V_{\alpha\beta}\begin{bmatrix} \cos(\omega t) & \sin(\omega t) \\ -\sin(\omega t) & \cos(\omega t) \end{bmatrix}$$

$$V_{dq2} = V_{\alpha\beta}\begin{bmatrix} -\cos(\omega t) & -\sin(\omega t) \\ \sin(\omega t) & -\cos(\omega t) \end{bmatrix}$$

$$V_{dq1} = V_1\begin{bmatrix} \cos(\varphi_1) \\ \sin(\varphi_1) \end{bmatrix} + V_2\begin{bmatrix} \cos(\varphi_2) & \sin(\varphi_2) \\ -\sin(\varphi_2) & \cos(\varphi_2) \end{bmatrix}\begin{bmatrix} \cos(2\omega t) \\ \sin(2\omega t) \end{bmatrix}$$

$$V_{dq1} = V_1 \begin{bmatrix} \cos(\varphi_1) \\ \sin(\varphi_1) \end{bmatrix} + V_{d2} \begin{bmatrix} \cos(2\omega t) \\ -\sin(2\omega t) \end{bmatrix} + V_{q2} \begin{bmatrix} \sin(2\omega t) \\ \cos(2\omega t) \end{bmatrix}$$

$$V_{dq2} = V_2 \begin{bmatrix} \cos(\varphi_1) \\ \sin(\varphi_1) \end{bmatrix} + V_{d1} \begin{bmatrix} \cos(2\omega t) \\ -\sin(2\omega t) \end{bmatrix} + V_{q1} \begin{bmatrix} \sin(2\omega t) \\ \cos(2\omega t) \end{bmatrix}$$

The DDSRF theory reference signals are computed for UPFC as shown below,

$$P_0 = \frac{3}{2}\begin{bmatrix} V_{d1} - V_{q1} - V_{d2} V_{q2} \end{bmatrix} \begin{bmatrix} i_{q2} \\ i_{d2} \\ i_{q1} \\ i_{d1} \end{bmatrix}$$

$$Q_0 = P_2 = \frac{3}{2}\begin{bmatrix} V_{d1} V_{q1} V_{d2} V_{q2} \end{bmatrix} \begin{bmatrix} i_{d2} \\ i_{q2} \\ i_{d1} \\ i_{q1} \end{bmatrix}$$

System Parameters

Comments	Value
UPFC	100 MVA
Line L1	Double circuit, 230 KV, 65Km
Line L2	50 Km, 500KV
Line L3	50 Km, 500KV
Transformer banks T1	1000MVA, 500KV/230KV
Transformer banks T2	800MVA, 500KV/230KV
Voltage buses B1 and B4	500KV
Voltage buses B2, B3, and B5	230KV
Load at bus B5	500KV,15000MVA
Load at bus B3	500KV, 200M
Power plant 1	13.8KV, 1000MVA
Power plant 2	13.8KV, 1200MVA

In the MATLAB environment, the suggested converter's findings are validated. Monitoring the capacitor's starting Vdc and determining the margin of error—the difference between the measured and reference Vdc—are the tasks of the DC potential control system. This error

serves as a source for the controller for PI, which calculates the real Vdc deviance. The actual part of UPFC-drawn flows is referenced using the controller yield. The measured values are compared to the two standard errors in a connected controller on the opposite side. Consequently, PI controller monitors and maintains a constant capacitor potential.

RESULTS

The 500 kV distribution system's Universal Energy Flow Controller (UPFC), which manages the power flow, is designed and tested using MATLAB SIMULINK 2021a. The UPFC sets the current at bus B1 and the flow of active as well as reactive energy through bus B2. It is situated at the left terminal of the 75 km line L2 adjacent to both of the 500 kV buses B 1 and B 2. Dual GTO-based 100-MVA, three-level, 48-pulse translators make up the system. Buses B1 as well as B2 are connected in series, and bus B1 is where the second one shunts. A DC bus lets the shunt as well as serial adapters share power. The series converter can connect Line L2 in series up to 10% of the standard lines-to-ground voltage, which is 28.87 kV.

For simulated DC link voltage of a UPFC, Simulation was used to compare how well the HHO-PI and PI controls worked. simulation's findings, shown in Fig. 4 and Table 1, unequivocally show that the HHO-PI controller works better than the PI controller. The HHO-PI controller has increased transient responsiveness, resilience, and adaptability to various operating situations. It also has improved optimisation capabilities. It successfully reduces overshoot and settling time, improving voltage control and system performance as a whole. These results show that the HHO-PI controller may be more effective than the conventional PI controller in controlling the DC link voltage of a UPFC.

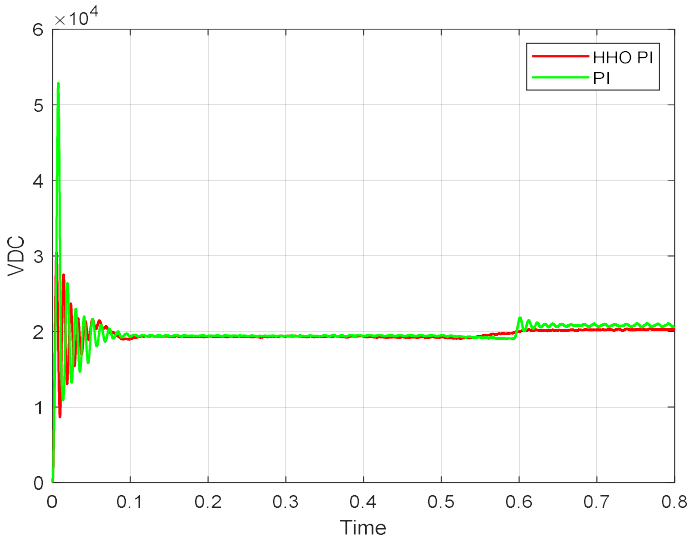

Figure 4 simulation plot

Table 1 HHO-PI Controller

Parameter	HHO	PI

Overshoot (%)	204.4%	243.45%
Settling time	0.1	0.1
Slew rate	6.120 (/µs)	5.370 (/µs)
Fall time	989.645 (/µs)	1.107 (ms)
Raise time	986.237 (/µs)	1.170 (ms)

The suggested HHO-PI controller, when compared to the standard PI controller, shows the capacity to seamlessly achieve active and reactive power references in addition to its improved performance in controlling the DC link voltage. The hybrid optimisation technique used by the HHO-PI controller allows it to dynamically modify its settings and optimise its performance in accordance with the supplied power references. The UPFC system's active and reactive power flow can be more precisely and accurately controlled because to its flexibility. The recommended controller as a result offers more reliable and slick monitoring of both reactive and active power references, enhancing power flow control and system stability.

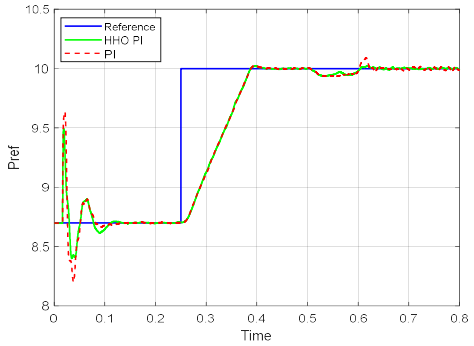

Figure 5 Active power

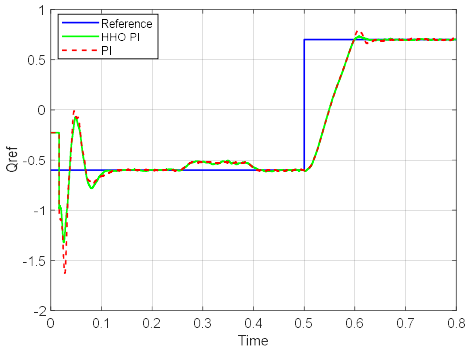

Figure 6 Reactive power

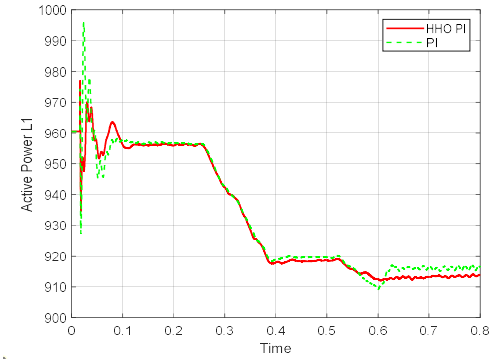

Figure 7 Active power of Line 1

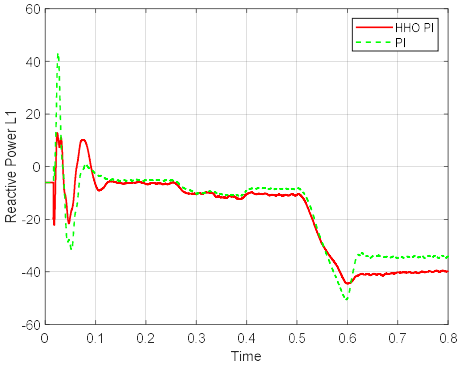

Figure 8 Reactive power of Line 1

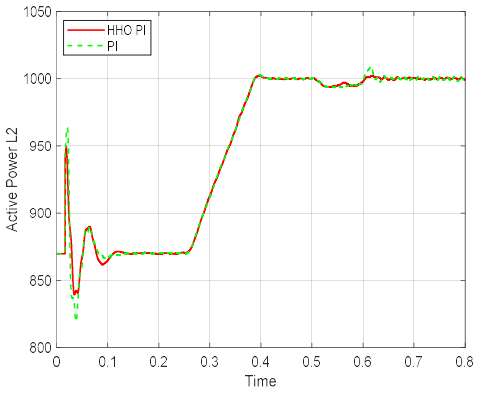

Figure 9 Active power of Line 2

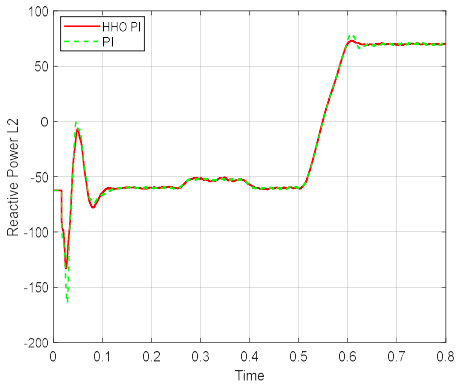

Figure 10 Reactive power of Line 2

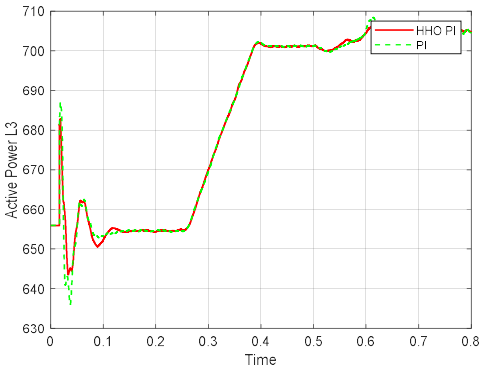

Figure 11 Active power of Line 3

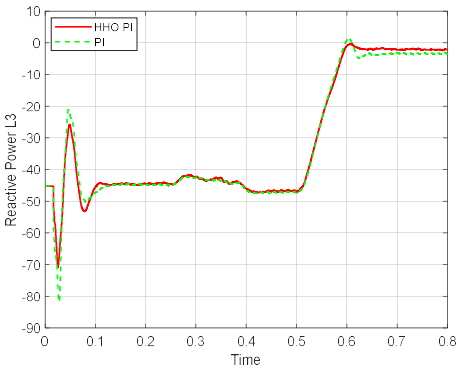

Figure 12 Reactive power of Line 3

The suggested HHO-PI controller has a number of advantages over the traditional PI controller, including greater service quality, superior performance in terms of DC link voltage management, and establishing smooth active and reactive power references. The comparison of Total Harmonic Distortion (THD) readings at the load side bus lends credence to this conclusion. According to the findings, the PI controller's THD value is 1.37% and the HHO-PI controller's is 0.88%. THD, a metric for waveform distortion, is used to evaluate the reliability of electrical power. A power source that is cleaner and more reliable will have a lower THD rating. It is obvious that the suggested controller offers higher-quality service since the HHO-PI controller exhibits a much lower THD value than the PI controller. The HHO-PI controller's improved power quality results in less voltage fluctuations, lower harmonic distortions, and more stability at the load side bus. These elements help the power system run more consistently and effectively, which improves the service quality overall. Therefore, based on the measured THD values, it can be said that the HHO-PI controller outperforms the traditional PI controller in terms of power quality.

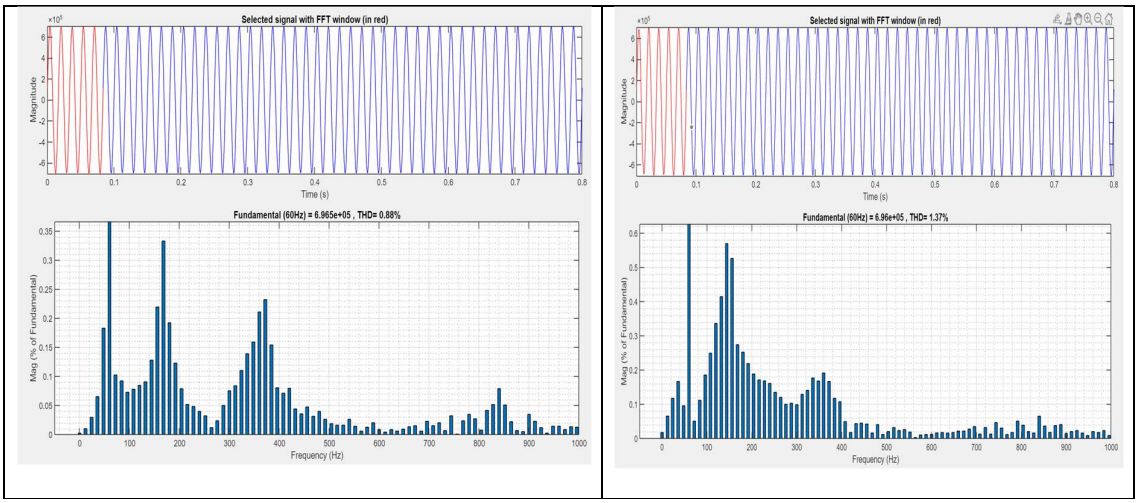

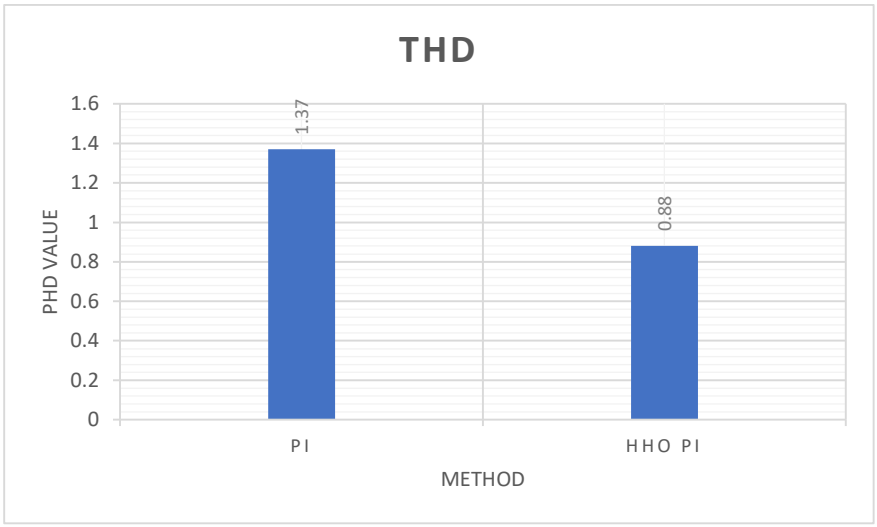

Figure 13comparison of total harmonic distortion

Conclusion:

Finally, this research study compares the performance of two controllers, HHO-PI and PI, in order to manage the simulated DC link voltage of a (UPFC). findings unequivocally show that the HHO-PI controller beats the PI controller in a number of key areas. The hybrid harmony search optimisation method of the HHO-PI controller, for starters, gives it improved optimisation capabilities. This enhances transient responsiveness and resilience, enabling the controller to swiftly adjust to changing operating circumstances and maintain a steady DC link voltage. In addition, the HHO-PI controller offers smoother monitoring of active and reactive power references, offering more precise control of power flow within the UPFC system. By doing this, system stability and better control of power flow are improved. Furthermore, compared to the PI controller, the HHO-PI controller produces notably reduced Total Harmonic Distortion (THD) values at the load sidebus. The lower THD number indicates better power quality, with fewer harmonic distortions and voltage swings, leading to a greater level of service. Overall, the study's findings demonstrate that the proposed HHO-PI controller works better than the conventional PI controller in regards to controlling the quantity of reactive and active electricity as well as the quality of power and regulating the DC connection's voltage.

Because of its hybrid optimisation technique, the HHO-PI controller is a more effective and economical controller for UPFC systems. It also tracks power references more smoothly and has lower THD values. These findings support enhanced performance, stability, and power quality in control techniques for power system applications. Additional optimisations may be investigated, and the use of hybrid optimisation algorithms might be expanded as a result of more in-depth study and development in this field, improving the regulation of power flow in UPFC systems.

References

Alabool, H. M., Alarabiat, D., Abualigah, L., & Heidari, A. A. (2021). Harris hawks optimization: a comprehensive review of recent variants and applications. In *Neural Computing and Applications* (Vol. 33, Issue 15). Springer London. https://doi.org/10.1007/s00521-021-05720-5

Alexander Jeevanantham, Y., & Srinath, S. (2022). ANN Based Reduced Switch Multilevel Inverter in UPQC for Power Quality Improvement. *Intelligent Automation and Soft Computing*, *33*(2), 909–921. https://doi.org/10.32604/iasc.2022.022907

Choudhury, S., Bajaj, M., Dash, T., Kamel, S., & Jurado, F. (2021). Multilevel inverter: A survey on classical and advanced topologies, control schemes, applications to power system and future prospects. *Energies*, *14*(18). https://doi.org/10.3390/en14185773

Debnath, S., Qin, J., Bahrani, B., Saeedifard, M., & Barbosa, P. (2015). Operation, control, and applications of the modular multilevel converter: A review. *IEEE Transactions on Power Electronics*, *30*(1), 37–53. https://doi.org/10.1109/TPEL.2014.2309937

Gade, S., Agrawal, R., & Munje, R. (2021). Recent trends in power quality improvement: Review of the unified power quality conditioner. *ECTI Transactions on Electrical Engineering, Electronics, and Communications*, *19*(3), 268–288. https://doi.org/10.37936/ecti-eec.2021193.244936

Gupta, A. (2022). Power quality evaluation of photovoltaic grid interfaced cascaded H-bridge nine-level multilevel inverter systems using D-STATCOM and UPQC. *Energy*, *238*, 121707. https://doi.org/10.1016/j.energy.2021.121707

He, H., Li, Z., Si, T., & Sun, L. (2019). Research on digital phase locked method in PWM rectifier. *Proceedings of 2019 IEEE 8th Joint International Information Technology and Artificial Intelligence Conference, ITAIC 2019*, *Itaic*, 1866–1870. https://doi.org/10.1109/ITAIC.2019.8785879

Heenkenda, A., Elsanabary, A., Seyedmahmoudian, M., Mekhilef, S., Stojcevski, A., & Aziz, N. F. A. (2023). Unified Power Quality Conditioners Based Different Structural Arrangements: A Comprehensive Review. *IEEE Access*, *11*(April), 43435–43457. https://doi.org/10.1109/ACCESS.2023.3269855

Kamal, S., Sayeed, F., Ahanger, T. A., Subbalakshmi, C., Kalidoss, R., Singh, N., & Nuagah, S. J. (2022). Particle Swarm Optimization and Modular Multilevel Converter Communication in Electrical Applications with Machine Learning Algorithm. *Computational Intelligence and Neuroscience*, *2022*. https://doi.org/10.1155/2022/8516928

Meral, M. E., & Çelík, D. (2019). A comprehensive survey on control strategies of distributed

generation power systems under normal and abnormal conditions. *Annual Reviews in Control*, *47*(xxxx), 112–132. https://doi.org/10.1016/j.arcontrol.2018.11.003

Patel, G. A., & Talari, M. K. (2021). *Performance Analysis And Power Quality Enhancement In Grid- Connected Solar PV-Wind Hybrid System*. *18*(5), 2629–2646.

Perez, M. A., Ceballos, S., Konstantinou, G., Pou, J., & Aguilera, R. P. (2021). Modular Multilevel Converters: Recent Achievements and Challenges. *IEEE Open Journal of the Industrial Electronics Society*, *2*(December 2020), 224–239. https://doi.org/10.1109/OJIES.2021.3060791

Reddy, C. R., Goud, B. S., Aymen, F., Rao, G. S., & Bortoni, E. C. (2021). Power quality improvement in hres grid connected system with fopid based atom search optimization technique. *Energies*, *14*(18). https://doi.org/10.3390/en14185812

Roknuzzaman, M., Yamaji, T., Nakata, H., & Hamasaki, S. I. (2020). Power Flow Control using Modular Multilevel Converter with circulating current control for 3-phase AC/AC Conversion. *23rd International Conference on Electrical Machines and Systems, ICEMS 2020*, 597–602. https://doi.org/10.23919/ICEMS50442.2020.9290877

Thamizh Thentral, T. M., Jegatheesan, R., & Subramani, C. (2021). New PQ theory for power quality improvement using modular multilevel converter based UPFC system. *Journal of Intelligent and Fuzzy Systems*, *40*(4), 7653–7665. https://doi.org/10.3233/JIFS-189584

Thentral, T. M. T., Palanisamy, R., Usha, S., Vishnuram, P., Bajaj, M., Sharma, N. K., Khan, B., & Kamel, S. (2022). The Improved Unified Power Quality Conditioner with the Modular Multilevel Converter for Power Quality Improvement. *International Transactions on Electrical Energy Systems*, *2022*. https://doi.org/10.1155/2022/4129314

Tripathy, B. K., Reddy Maddikunta, P. K., Pham, Q. V., Gadekallu, T. R., Dev, K., Pandya, S., & Elhalawany, B. M. (2022). Harris Hawk Optimization: A Survey onVariants and Applications. *Computational Intelligence and Neuroscience*, *2022*. https://doi.org/10.1155/2022/2218594

Xiu, L., Du, Z., Wu, B. B., Li, G., Wang, D., & Song, H. (2021). A novel adaptive frequency extraction method for fast and accurate connection between inverters and microgrids. *Energy*, *221*, 119795. https://doi.org/10.1016/j.energy.2021.119795

Zeng, R., & Xu, L. (n.d.). *11_201X_Statcom_Design*. 1–10.